

Sensitivity of the FACET experiment to Heavy Neutral Leptons and Dark Scalars

Maksym Ovchynnikov,^{a,b} Viktor Kryshtal,^c Kyrilo Bondarenko^{d,e,f}

^a*Instituut-Lorentz, Leiden University, Niels Bohrweg 2, 2333 CA Leiden, The Netherlands*

^b*Institut für Astroteilchen Physik, Karlsruher Institut für Technologie (KIT), Hermann-von-Helmholtz-Platz 1, 76344 Eggenstein-Leopoldshafen, Germany*

^c*Department of Physics, Taras Shevchenko National University of Kyiv, 64 Volodymyrs'ka str., Kyiv 01601, Ukraine*

^d*IFPU, Institute for Fundamental Physics of the Universe, via Beirut 2, I-34014 Trieste, Italy*

^e*SISSA, via Bonomea 265, I-34132 Trieste, Italy*

^f*INFN, Sezione di Trieste, SISSA, Via Bonomea 265, 34136, Trieste, Italy*

E-mail: maksym.ovchynnikov@kit.edu, victor.kryshtal@gmail.com,
kyrylo.bondarenko@sissa.it

ABSTRACT: We analyze the potential of the recently proposed experiment FACET (Forward-Aperture CMS ExTension) to search for new physics. As an example, we consider the models of Higgs-like scalars with cubic and quartic interactions and Heavy Neutral Leptons. We compare the sensitivity of FACET with that of other proposed “intensity frontier” experiments, including FASER2, SHiP, etc. and demonstrate that FACET could probe an interesting parameter space between the current constraints and the potential reach of the above mentioned proposals.

Contents

| | | |
|----------|--|-----------|
| 1 | Introduction | 1 |
| 2 | Portals | 3 |
| 2.1 | Scalar portal with the quartic coupling | 3 |
| 2.2 | Heavy Neutral Leptons | 3 |
| 3 | FACET experiment | 4 |
| 4 | FACET vs FASER2: qualitative comparison of the sensitivity | 6 |
| 4.1 | Scalar portal | 7 |
| 4.1.1 | Geometric acceptance | 7 |
| 4.1.2 | Maximal number of events | 10 |
| 4.2 | Comparison for HNLs | 11 |
| 5 | Results and discussion | 13 |
| 6 | Conclusions | 14 |
| A | Mixing and quartic coupling at the lower bound of the sensitivity | 15 |

1 Introduction

Despite its success in describing accelerator data, the Standard model (SM) fails to explain several observed phenomena constituting beyond the Standard model problems: neutrino masses, dark matter, and the matter-antimatter asymmetry. These problems may be resolved by extending the SM particle content with some new particles. One class of extensions is where new particles interact with SM via renormalizable operators suppressed by very small couplings, the so-called portals. Depending on the spin of the mediator field entering the portal operator, there are three types of portals – scalar, vector, and fermion [1, 2].

To search for portal particles, many experiments have been proposed during the last few years. Examples include dedicated beam experiments such as SHiP [3], DUNE [4], SHADOWS [5], NA62 [6]; LHC-based experiments, such as MATHUSLA [7], Codex-b [8], ANUBIS [9], AL3X [10]. There is a class of LHC-based experiments that have decay volume covering large pseudorapidities, which is called the far-forward experiments. The particles produced in the far-forward direction have large energies, $E = \mathcal{O}(1 \text{ TeV})$, which means that their lifetime is increased by

$\gamma \sim 10^3(1 \text{ GeV}/m)$. Therefore, as compared with the off-axis experiments located at the same distance, the far-forward experiments may probe particles with shorter lifetimes.

The representatives of this class are already running FASER [11, 12], FASER ν [13, 14] and SND@LHC [15] experiments. Their proposed upgrades, FASER2/FASER ν 2 and AdvSND, would be installed at the Far Forward physics facility and work during the High Luminosity phase of the LHC [16]. Recently, a new far-forward experiment FACET has been proposed [17]. Apart from covering $\simeq 4$ times larger solid volume and having longer decay volume, it would be located in 100 meters downwards the CMS interaction point – $\simeq 5$ times closer than SND@LHC/FASER, and in this way allows to probe even shorter lifetimes [18, 19].

In this work, we estimate the sensitivity of the FACET experiment to models of scalar and fermion portals, making a qualitative comparison of its sensitivity with FASER2. The final results are shown in Fig. 1, where we also show the sensitivities of other proposed experiments such as SHiP, MATHUSLA, Belle II, and LHC, to demonstrate the possible synergy between these searches. We see that due to larger decay volume and closer distance from the interaction point, FACET allows to significantly extend the probed parameter space as compared to FASER2.

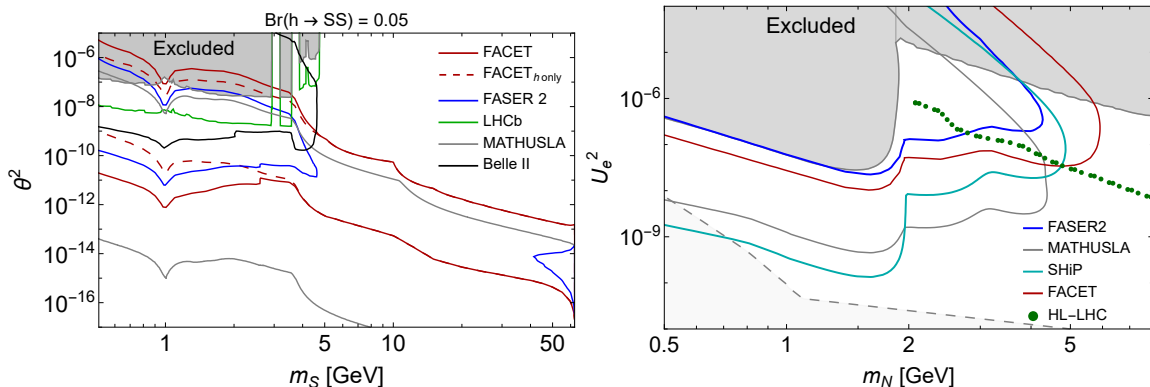


Figure 1. Sensitivity of FACET and FASER2 to the models of HNLs and Higgs-like scalars. Left panel: Higgs-like scalars, assuming $\text{Br}(h \rightarrow SS) = 0.05$. The solid red line shows the sensitivity of FACET including the production of scalars from h and B , while the dashed line denotes the sensitivity to scalars from h only. We also include the sensitivity of Belle II from [20] (see also [21]). Right panel: HNLs that mix predominantly with ν_e . For comparison, we also show the sensitivity of SHiP and MATHUSLA experiments from [2], as well as the optimistic estimate of the sensitivity of HL-LHC from [22]. The region excluded by the previous experiments is given from [23] for HNLs and from [2] for Higgs-like scalars.

The content of the paper is as follows. In Sec. 2, we briefly describe the scalar and neutrino portals. In Sec. 3, we describe the FACET experiment. In Sec. 4, we compare the reach of the FACET and FASER2 experiments based on semi-analytic estimates, considering scalars and heavy neutral leptons produced by decays of B

mesons and Higgs bosons. In Sec. 5, we discuss the obtained results and make their comparison with the literature. Finally, in Sec. 6, we make conclusions.

2 Portals

2.1 Scalar portal with the quartic coupling

The general form of the Lagrangian of the scalar portal below the electroweak scale [1] is

$$\mathcal{L}_{\text{scalar portal}} = \theta m_h^2 h S + \frac{\alpha}{2} h S S, \quad (2.1)$$

where h is the Higgs boson field, S is a new scalar particle (also called the Higgs-like scalar, or dark scalar), θ is the mixing angle, and α is the quartic coupling constant. The scalar with mass in GeV range may be a mediator between the SM and dark matter particles or serve as a light inflaton [24]. The phenomenology of the scalar portal at accelerator experiments has been intensively studied in [24–35] as well as in [36–45] in the context of the light Higgs boson.

At the LHC, Higgs bosons are copiously produced. In particular, during the high luminosity phase, around 10^8 bosons will be generated. In the case $\alpha \neq 0$, they may decay into a pair of scalars through the process $h \rightarrow SS$.

Current constraints on α are not very restrictive for the model of scalars. Indeed, the strongest bound on α comes from searches for invisible decays $h \rightarrow \text{inv}$ at ATLAS and CMS, constraining $\text{Br}(h \rightarrow \text{inv}) < 0.15$ [46, 47]. During the high luminosity phase of the LHC, it would be possible to probe the branching ratio down to the values $\text{Br}(h \rightarrow \text{inv}) = 0.05$ [48].

The number of Higgs bosons that would be produced during the High Luminosity phase of the LHC is $N_h \simeq 2 \cdot 10^8$. Therefore, given the current constraints on $\text{Br}(h \rightarrow \text{inv})$, the production channel $h \rightarrow SS$ allows to significantly extend the reach of the LHC and LHC-based experiments, making it possible to search for the scalars with masses up to $m_S \simeq m_h/2$.

The parameter space of dark scalars excluded by past experiments and probed by proposed LHC experiments (we choose FASER2 and MATHUSLA as a representative example), assuming $\text{Br}(h \rightarrow SS) = 0.05$, is shown in the left panel of Fig. 1. In the paper [49], it has been demonstrated that FASER2 has a limited potential to probe this model, mainly due to the suppressed small angular coverage and short length of the decay volume.

2.2 Heavy Neutral Leptons

The Lagrangian of the fermion portal is

$$\mathcal{L}_f = F_{\alpha I} \bar{L}_\alpha \tilde{H} \mathcal{N}_I + \text{h.c.} + \mathcal{N} \text{ mass term}, \quad (2.2)$$

where $\mathcal{N}_I, i = 1, 2, \dots$ is a massive fermion (that may be either Dirac or Majorana depending on the \mathcal{N} mass term), $\tilde{H} = i\sigma_2 H^*$ is the Higgs doublet in the conjugated representation, L_α is the SM lepton doublet ($\alpha = e, \mu, \tau$), and $F_{\alpha I}$ are complex couplings. Below the scale of the electroweak symmetry breaking, the first term in (2.2) induces a mass mixing between the \mathcal{N} and active neutrinos. The mixing is parametrized by the mixing angle $U_{\alpha I} = F_{\alpha I}/\sqrt{2}v \ll 1$, where v is the Higgs VEV. As a result, the combination of active neutrinos $\sum_\alpha F_{\alpha I}$ and the fermion \mathcal{N}_I are a combination of two mass eigenstates – a very light neutrino and a heavy neutral lepton N_I (HNL).

The mass mixing determines the way how HNLs interact with SM particles. Similarly to the interaction of the SM active neutrinos, it is with other neutrinos and charged leptons via W and Z bosons. The only difference is that the HNL couplings are suppressed by $U_{\alpha I}$.

The parameter space of HNLs is shown in the right panel of Fig. 1. We show SHiP, FASER2, MATHUSLA, and high luminosity LHC among the proposed experiments. At the LHC, HNLs heavier than kaons may be produced in decays of D, B mesons, and W bosons. The last channel allows extending the maximal HNL mass reach from $m_N = m_B \simeq 5$ GeV to $m_N \simeq m_W$ as compared to the dedicated beam experiments such as SHiP. However, this is not the case for either MATHUSLA or FASER2, since they are located too far from the HNL production point, and the HNLs produced from W bosons in the accessible parameter space are too short-lived to reach the decay volume [50].

3 FACET experiment

FACET (Forward Aperture CMS ExTension) [17] is a recent proposal of a subsystem of CMS to be added to search for long-lived particles during the High Luminosity (HL) phase of the LHC.

The schematic layout of FACET is shown in Fig. 2. Given z as the distance from the CMS experiment along the beam axis, FACET will be located between the 35 T·m superconducting beam separation dipole D1 at $z = 80$ m and the TAXN absorber at $z = 128$ m. The decay volume is an enlarged proton beam pipe with radius $r = 0.5$ m located from $z = 101$ m to $z = 119$ m.

The detector part is located right after the decay volume. It has shape of the annulus with the inner radius $r_{\text{in}} = 18$ cm and outer radius $r_{\text{out}} = 50$ cm. The detector covers polar angles $1.5 < \theta < 4$ mrad and consists of $\simeq 3$ m of silicon tracker with the transversal resolution of $\sigma_{x,y} = 30$ μm , the timing layer with Low-Gain Avalanche Detectors (LGAD) having resolution $\sigma_t \sim 30$ ps, and a high granularity EM and hadronic calorimeter.

The background is greatly reduced because of 200-300 λ_{int} of magnetized iron in the LHC quadrupole magnets Q1–Q3. Detailed FLUKA simulations predict

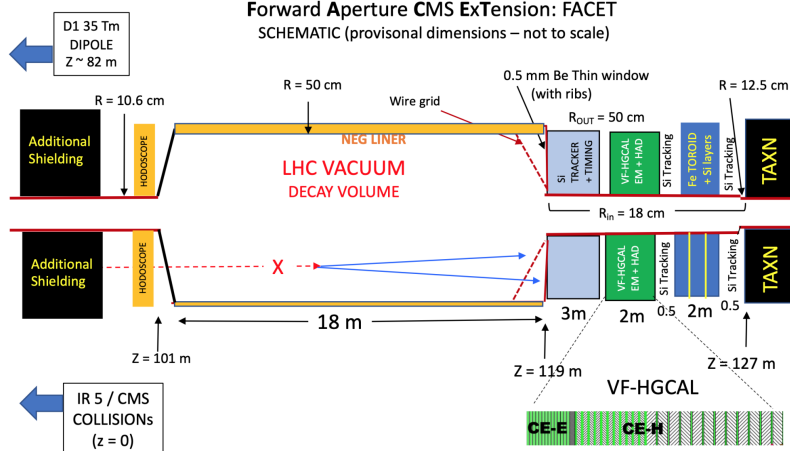


Figure 2. The schematic layout of the FACET experiment (see text for details). The figure is taken from [17].

$\simeq 30$ charged particles with momentum $p > 1$ GeV and $\simeq 1$ light neutral hadron (K_S^0, K_L^0, Λ) per bunch crossing [17]. Charged particles and decays of neutral hadrons may mimic decays of new physics particles. The combination of the precision hodoscope (with the inefficiency of 10^{-5}) and precision tracking reduces the background for most of the new physics decay channels down to a negligible level for the mass of a new physics particle $m_X \gtrsim 0.8$ GeV. Nevertheless, decays of neutral hadrons create a background in the region $m_X \lesssim 0.8$ GeV, making searching for new particles in this mass range complicated.

However, given the specific model, the background may be greatly reduced. First, one may utilize specific final states of decays of the HNLs and dark scalars, see [25, 51] for detail. In particular, the neutral SM particles do not decay (or decay very rarely) into solely a dilepton pair [52]. In contrast, these may be the main decay modes of light scalars (the decay $S \rightarrow l^+l^-$) and the HNLs (decays $N \rightarrow l^+l'^-\nu$, $N \rightarrow \pi^+l^-$). The only caveat is the situation when the decay product would be falsely reconstructed (in particular). In addition, in the case of dark scalars and HNLs with masses up to $\mathcal{O}(1$ GeV), most of their decays (into l^+l^- , $\pi^+\pi^-$, $N \rightarrow \pi^+l^-$) – are fully reconstructable. Therefore, the invariant mass distribution is peaked at the true scalar/HNL mass. Collecting even a few of such events would be enough to distinguish them from similar events from decays of neutral particles, for which the distribution is peaked at m_{K^0} (a very rare process $K \rightarrow \pi^+\pi^-$) or is continuous (the decay $K \rightarrow \pi^-l^+\bar{\nu}$).

4 FACET vs FASER2: qualitative comparison of the sensitivity

In this section, we compare the sensitivities of the FACET and FASER2 experiments. For this purpose, we will use semi-analytic estimates similar to the ones presented in [50].

We estimate the number of events with decays of a particle $Y = S, N$ at the FACET and FASER2 experiments (see Table 1) in the following way:

$$N_{\text{events}} = \sum_X N_X \times \chi_{S/N}^{(X)} \cdot \text{Br}(X \rightarrow Y) \times \int \frac{dP_{\text{decay}}(\gamma_Y, z)}{dz} f_{\theta_Y, E_Y} \cdot \epsilon_{\text{decay}}(\gamma_Y, \theta_Y, z) d\theta_Y dE_Y dz \quad (4.1)$$

Here, X corresponds to the decaying particle that produces scalars, with N_X being the total number of SM particles produced during the high luminosity phase of the LHC. We assume $N_h = 1.7 \cdot 10^8$ from [53], take $N_B = 2.4 \cdot 10^{15}$, $N_D = 5 \cdot 10^{16}$, from FONLL [54–57] at the upper bound of uncertainties (see a discussion in [50]), and $N_W = 3.3 \cdot 10^{11}$ from [58].

$\chi_Y^{(X)} = 1$ or 2 is the number of particles Y produced per decay of X .

The integration in (4.1) is performed over Y energies E_Y , polar angles θ_Y , and the distance from the collision point along the beam axis z within $l_{\text{min}} < z < l_{\text{min}} + l_{\text{fid}}$, where l_{min} is the distance to the beginning of the decay volume, and l_{fid} is the decay volume length. $dP_{\text{decay}}/dz = \frac{e^{-z/c\tau_Y\gamma_Y}}{c\tau_Y\gamma_Y}$ is the differential decay probability.

$f_{\theta_Y, E_Y}^{(X)}$ is the angle-energy distribution of Y produced by decays of X . To derive it, we have followed the semi-analytic approach summarized in [49]; namely, we have integrated the differential distribution $d\text{Br}(X \rightarrow Y)$ multiplied with the distribution of the mother particle X over X energy and angles. The mother particle distributions have been obtained from FONLL [54–57] (B, D), by the method described in [49] (for h), and from [59] (for W).

$\epsilon_{\text{decay}}(\gamma_S, \theta_S, z)$ is the decay acceptance – the fraction of decay products from Y intersecting the front plane of the detector. We estimate it using a simple Monte Carlo simulation by approximating the decay of scalars into two massless particles, and of HNLs into three massless particles via the charged current.¹

Further, we will assume that both FACET and FASER2 are background-free experiments. Taking into account considerable background from neutral hadron decays on FACET for $m_Y \lesssim 0.8$ GeV, discussed in Section 3, the obtained results for FACET are only valid above this mass. Parameters of the experiments are summarized in Table 1.

Let us compare the sensitivity of FACET and its modification at the lower bound (the regime $c\tau_Y\gamma_Y \gg l_{\text{max}}$) and the upper bound (regime $c\tau_Y\gamma_Y \lesssim l_{\text{min}}$) with the

¹The approximation works within 25% accuracy for the whole scalar/HNL mass range.

| Experiment | l_{\min} , m | l_{fid} , m | $\theta_{\min}, \theta_{\max}$, mrad | Ω , sr |
|------------|----------------|----------------------|---------------------------------------|---------------------|
| FASER2 | 480 | 5 | 0, 2.1 | $1.3 \cdot 10^{-5}$ |
| FACET | 101 | 18 | 1.6, 4.1 | $4.5 \cdot 10^{-5}$ |

Table 1. Parameters of FASER2 and FACET configurations: the distance to the beginning of the decay volume l_{\min} , the length of the decay volume l_{fid} , the polar angle coverage of detectors $\theta_{\min}, \theta_{\max}$, and the solid angle Ω covered by the detectors.

sensitivity of FASER2. The lifetime scales as $\tau_Y \propto g_Y^{-2}$, where g_Y is the mixing angle. The production branching ratio scales as Br

At the upper bound, the number of events behaves as $N_{\text{events}} \propto g_Y^2 \times \exp[-l_{\min}/c\tau_Y\gamma_Y]$. Therefore, neglecting the power g_Y^2 , for ratio of the maximal probed mixing angles we get

$$\frac{g_{\text{upper,FACET}}^2}{g_{\text{upper,FASER2}}^2} \simeq \frac{l_{\min}^{\text{FASER2}}}{l_{\min}^{\text{FACET}}} \cdot \frac{\langle \gamma_Y \rangle_{\text{FACET}}}{\langle \gamma_Y \rangle_{\text{FASER2}}} \approx 5, \quad (4.2)$$

given ≈ 5 times smaller l_{\min} at FACET and $\langle \gamma_Y \rangle_{\text{FACET}} \approx \langle \gamma_Y \rangle_{\text{FASER2}}$.

At the lower bound, $e^{-z/c\tau_Y\gamma_Y} \approx 1$, and the ratio of the probed mixing angles is

$$\frac{g_{\text{lower,FACET}}^2}{g_{\text{lower,FASER2}}^2} \approx \left(\frac{\epsilon_{\text{geom}}^{\text{FASER2}}}{\epsilon_{\text{geom}}^{\text{FACET}}} \times \frac{l_{\text{det}}^{\text{FASER2}}}{l_{\text{det}}^{\text{FACET}}} \right)^\kappa, \quad (4.3)$$

Here, $\kappa = 1/2$ in the case when both Y production and decay are controlled by θ , and $\kappa = 1$ in the case when the production is controlled by different couplings. ϵ_{geom} is the averaged geometric acceptance at the lower bound:

$$\epsilon_{\text{geom}} \approx \frac{1}{l_{\text{det}}} \int f_{\theta_Y, E_Y} \cdot \epsilon_{\text{decay}}(\gamma_Y, \theta_Y, z) d\theta_Y dE_Y dz \quad (4.4)$$

4.1 Scalar portal

The production processes of scalars at the LHC are $h \rightarrow S + S$ for the Higgs bosons, and $B^{+/0} \rightarrow S + S + X_s$, $B_s \rightarrow S + S$, $B^{+/0} \rightarrow S + X_s$, for the B mesons [25], see also Fig. 3. The first three processes are mediated by the quartic coupling α , while the process $B^{+/0} \rightarrow S + X_s$ by the mixing angle θ .

4.1.1 Geometric acceptance

Let us discuss the geometric acceptance. For the moment, we will drop the decay acceptance.

The solid angle distribution $df/d\cos(\theta) \sim df/d\Omega$ of Higgs bosons, B mesons, and light scalars produced in their decays is shown in Fig. 4. The distribution of B, h remains constant in the angular coverage of FASER2 and gradually drops by a factor 1.5-2 for the angular coverage of the FACET experiment. While the distribution of scalars with mass close to the kinematic threshold is the same as for their mother

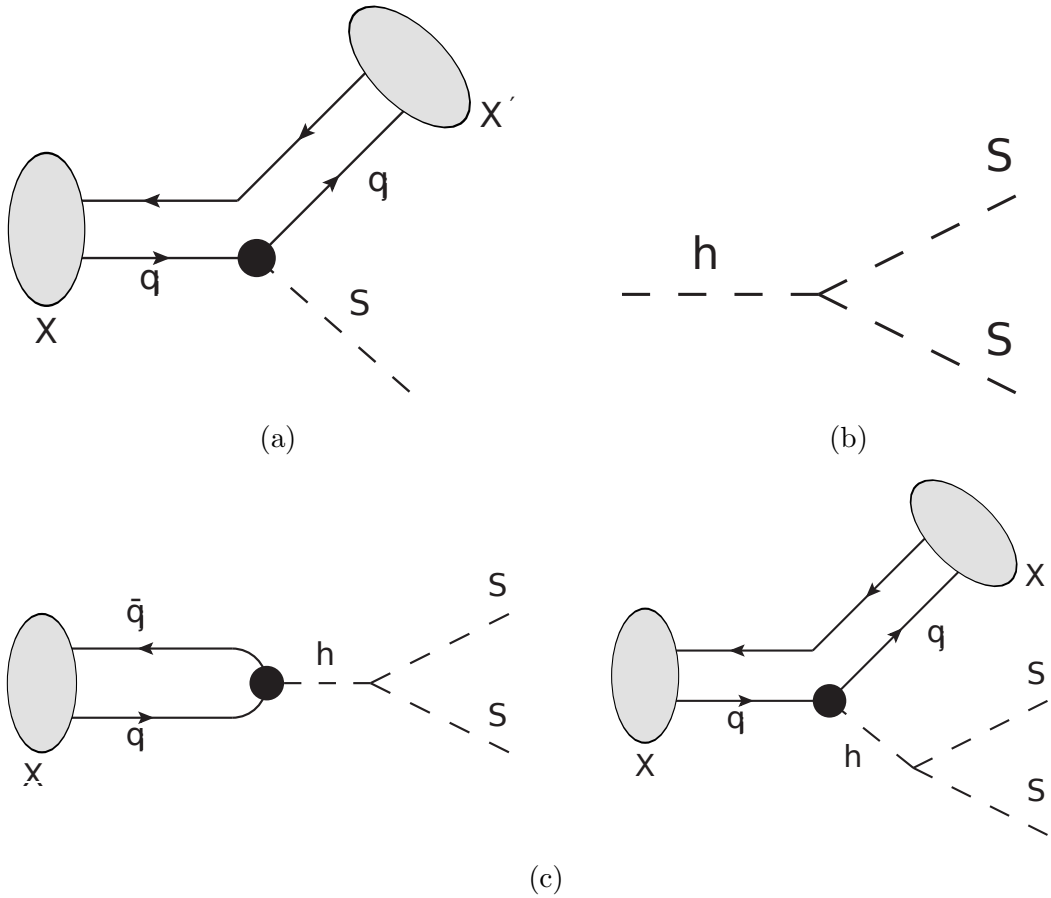


Figure 3. Diagrams of the production of the scalar S in the model (2.1): meson decay $X \rightarrow X' + S$ (a) mediated by the mixing θ ; and the Higgs boson decay $h \rightarrow S + S$ (b), the mesons decays $X \rightarrow S + S$, $X \rightarrow X' + S + S$ (c) mediated by the quartic coupling α .

particles, the distribution of light scalars $m_S \ll m_B, m_h/2$ gets broadened due to acquiring transverse momentum, of order of $p_T \simeq m_{B/h}/2$. Given that the typical B, h energy in the far-forward direction is $\mathcal{O}(1 \text{ TeV})$, the smearing is $\Delta\theta \sim p_T/1 \text{ TeV}$ – smaller than the angular coverage of FACET and FASER2 for scalars from B mesons, and much larger for scalars from h . As a result, the angular distribution of light scalars from B remains very similar to the distribution of B , while in the case of scalars from h it is isotropic up to the angles 30 mrad. This in particular suggests that FACET already has an optimal placement and size to search for particles from B mesons.

Therefore, if not including the decay acceptance in Eq. (4.4), for the geometric acceptance of scalars from $X = h, B$ one has

$$\frac{\epsilon_{\text{geom},S}^{\text{FACET}}}{\epsilon_{\text{geom},S}^{\text{FASER2}}} \approx \begin{cases} \Omega_{\text{FACET}}/\Omega_{\text{FASER2}}, & m_S \ll m_B, m_h/2 \\ \epsilon_{\text{geom},X}^{\text{FACET}}/\epsilon_{\text{geom},X}^{\text{FASER2}}, & m_S \rightarrow m_B \text{ or } m_h/2 \end{cases} \quad (4.5)$$

Let us now discuss the effect of the decay acceptance. It becomes important

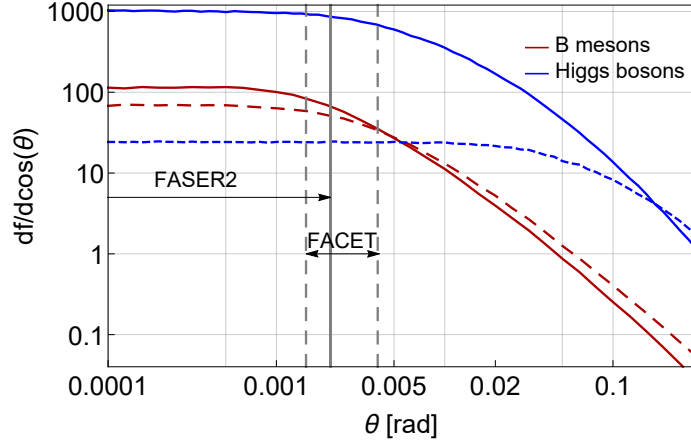


Figure 4. The solid angle distribution $df/d\cos(\theta) \sim df/d\Omega$ of B mesons, Higgs bosons (solid lines) and light scalars with $m_S = 50$ MeV produced by their decays (dashed lines). The arrows indicate polar angle coverage of FASER2 and FACET experiments.

| Experiment | $\epsilon_{\text{geom},S}, h \rightarrow SS$ | | $\epsilon_{\text{geom},S}, B \rightarrow KS$ | |
|------------|--|---------------------|--|---------------------|
| | $m_S = 50$ MeV | $m_S = 62$ GeV | $m_S = 50$ MeV | $m_S = 5.1$ GeV |
| FASER2 | $5 \cdot 10^{-5}$ | $1 \cdot 10^{-3}$ | $2.8 \cdot 10^{-3}$ | $7.5 \cdot 10^{-3}$ |
| FACET | $1.7 \cdot 10^{-4}$ | $6.1 \cdot 10^{-4}$ | $6.9 \cdot 10^{-3}$ | $1 \cdot 10^{-2}$ |

Table 2. Geometric acceptances (Eq. (4.4) for scalars produced by decays of Higgs bosons and B mesons, for various choices of the scalar mass.

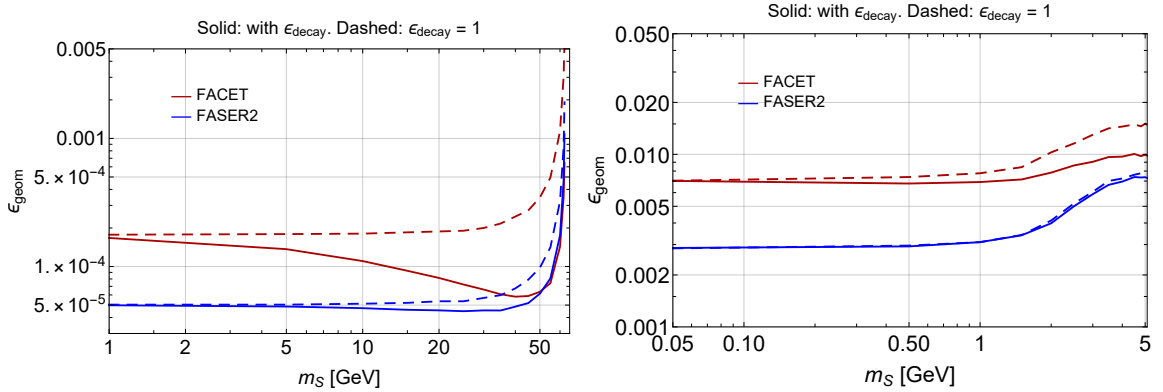


Figure 5. The behavior of the geometric acceptance (4.4) for scalars produced in decays $h \rightarrow SS$ and $B \rightarrow X_S + S$. The solid lines are obtained with taking the decay acceptance, ϵ_{decay} , into account, whereas the dashed lines correspond to $\epsilon_{\text{decay}} = 1$.

if the characteristic angle between the decay products in a 2-body decay, $\langle \alpha \rangle \simeq 1 \arcsin(2/\gamma_S)$, exceeds the angle covered by the detector as seen from the beginning of the decay volume, which is 0.4 rad for FASER2 and 0.1 rad for FACET.

Given the typical scalar energies $E_S = \mathcal{O}(1 \text{ TeV})$, for light scalars with $m_S \ll m_{h/2}, m_B$ the decay acceptance is 1. However, with the increase of the scalar mass,

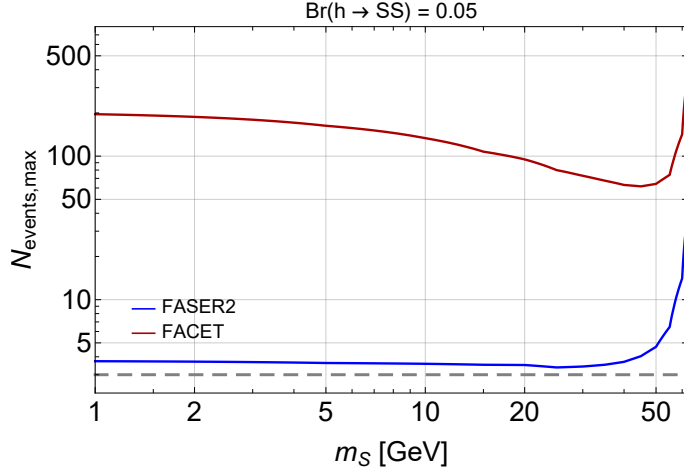


Figure 6. The maximal possible number of events (eq. (4.8)) at FASER2 and FACET as a function of the scalar mass. The dashed gray line denotes 3 events defining the sensitivity domain of the experiments.

more and more decay products produced in the beginning of the decay volume fly in directions outside the detector coverage. This feature effectively shrinks l_{det} . For FACET, this effect is much more important than for FASER2. As a result, in dependence on the scalar mass, the geometric acceptance at FACET drops even below the geometric acceptance at FASER2 for h and becomes very close to the geometric acceptance at FASER2 for B , see Fig. 5 and Table 2.

Given the ratio $l_{\text{det}}^{\text{FASER2}}/l_{\text{det}}^{\text{FACET}} \approx 4$ and the behavior of the geometric acceptances (see Fig. 5), we conclude that the overall increase of the number of events in the regime of the lower bound at FACET as compared to FASER2 reaches a factor 2 – 15 and 5 – 15 for the case of the production from h and B respectively, in dependence on the scalar mass.

4.1.2 Maximal number of events

In the case of the production from Higgs bosons, it is also useful to compare **the maximal possible number of events** at FACET and FASER2. An estimate with an accuracy in a factor of two is given by

$$N_{\text{events,max}} \approx N_h \cdot (2 \cdot \text{Br}(h \rightarrow SS)) \cdot \epsilon_{\text{geom}} \cdot P_{\text{decay,max}}, \quad (4.6)$$

where ϵ_{geom} is given by Eq. (4.4), while $P_{\text{decay,max}}$ is the maximal value of the decay probability as a function of $l_{\text{decay,S}} = c\tau_S\gamma_S$, which depends only on $l_{\text{min}}, l_{\text{max}}$:²

²In reality, the true maximal events number is even somewhat smaller, since for each given m_S, θ^2 there is the distribution in l_{decay} due to the energy distribution of scalars.

| Experiment | $\epsilon_{\text{geom}, D_s \rightarrow e + N}$ | $\epsilon_{\text{geom}, B_c \rightarrow e + N}$ | $\epsilon_{\text{geom}, W \rightarrow e + N}$ |
|------------|---|---|---|
| FASER2 | $8.5 \cdot 10^{-3}$ | $4.9 \cdot 10^{-3}$ | $4.2 \cdot 10^{-4}$ |
| FACET | $1.4 \cdot 10^{-2}$ | $1.3 \cdot 10^{-2}$ | $1.3 \cdot 10^{-3}$ |

Table 3. Geometric acceptances (4.4) for HNLs produced in decays of D_s, B_c , and W bosons (the decay acceptance is included). The HNL masses are $m_N = 1.5$ GeV for the production from D_s , 3 GeV for the production from B_c , and 5 GeV for the production from W .

$$P_{\text{decay,max}} = \left[\left(\frac{l_{\text{min}} + l_{\text{fid}}}{l_{\text{min}}} \right)^{-\frac{l_{\text{min}}}{l_{\text{fid}}}} - \left(\frac{l_{\text{min}} + l_{\text{fid}}}{l_{\text{min}}} \right)^{-\frac{l_{\text{min}} + l_{\text{fid}}}{l_{\text{fid}}}} \right] \approx \begin{cases} 3.8 \cdot 10^{-3}, & \text{FASER2,} \\ 0.06, & \text{FACET} \end{cases} \quad (4.7)$$

Plugging in all numbers, we get

$$N_{\text{events,max}} \approx \begin{cases} 3.8 \cdot \left(\frac{\epsilon_{\text{geom}}}{4.8 \cdot 10^{-5}} \right), & \text{FASER2,} \\ 200 \cdot \left(\frac{\epsilon_{\text{geom}}}{1.8 \cdot 10^{-4}} \right), & \text{FACET,} \end{cases} \quad (4.8)$$

see also Fig. 6.

From Eq. (4.8), we see that $N_{\text{events,max}}$ at FASER2 is very close to the number of events required at 95% C.L. to observe one event in background free regime. More accurate estimates [49] that included the energy distribution of scalars (which decreases the value of $P_{\text{decay,max}}$) showed that it is even lower, dropping below 3. This explains why FASER2 has no sensitivity to scalars from Higgs bosons in the domain $m_S \lesssim 45$ GeV.

4.2 Comparison for HNLs

Consider now the case of HNLs. The interaction vertices of HNLs with SM particles are similar to the vertices of active neutrinos ν_α , but are suppressed by the mixing angle $U_\alpha \ll 1$ [60, 61].

At the LHC, the HNLs may be copiously produced in decays of D, B mesons and W bosons [51]. In this Section, we consider HNLs that mix predominantly with ν_e , keeping in mind that the results for the other mixings are similar.

For the qualitative comparison, we will consider the following production channels: $D_s \rightarrow N + e$, $B_c \rightarrow N + e$, $W \rightarrow N + e$, which respectively dominate the production of HNLs from D mesons above $m_N \simeq 0.5$ GeV, from B mesons above $m_N \simeq 3$ GeV, and from W bosons. The angular distributions for these particles, as well as for light HNLs with mass $m_N = 50$ MeV produced by their decays, are shown in Fig. 7.

The values of the geometric acceptances are given in Table 3.

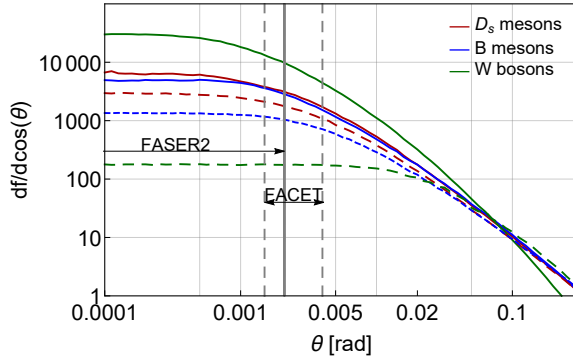


Figure 7. The angular distribution of D_s, B_c mesons, W bosons (solid lines), and light HNLs with $m_N = 50$ MeV produced by their decays (dashed lines). The arrows indicate the polar angle coverage of FASER2 and FACET experiments.

The production from W bosons is not important for the lower bound of the sensitivity of FACET and FASER2. To demonstrate this, let us consider two mass ranges $m_N \lesssim m_{B_c}$ and $m_N > m_{B_c}$. In the mass range $m_N \lesssim m_{B_c}$, the production from W competes with the production from D and B . Let us compare the total number of HNLs produced by B mesons and by W bosons for FACET (for FASER2, the situation is similar):

$$\frac{N_{\text{prod}}^{\text{from } W}}{N_{\text{prod}}^{\text{from } B}} = \frac{N_W \cdot \epsilon_{\text{geom}}^{\text{from } W}}{N_B \cdot \epsilon_{\text{geom}}^{\text{from } B}} \times \frac{\text{Br}(W \rightarrow N + e)}{\sum_i f_{b \rightarrow B_i} \text{Br}(B_i \rightarrow N + X)} \simeq \simeq 10^{-5} \times \frac{\text{Br}(W \rightarrow N + e)}{\sum_i f_{b \rightarrow B_i} \text{Br}(B_i \rightarrow N + X)} \ll 1 \quad (4.9)$$

where $f_{b \rightarrow B_i}$ is the fragmentation fraction of b quark into a meson B_i , and we have taken into account that the second multiplier remains $\ll 10^5$ for practically all HNL masses below m_{B_c} [50].

For the mass range $m_N > m_{B_c}$, HNLs from W are too short-lived and cannot reach the detector. Indeed, let us estimate the number of events with HNLs with mass m_{B_c} produced by W decays at $l_{\text{decay}} = c\tau_N \gamma_N \simeq l_{\text{min}}$. The number of events increases with decreasing l_{decay} for $l_{\text{decay}} \gtrsim l_{\text{min}}$, so this should give an upper bound of events from W for the lower bound of sensitivity. The corresponding mixing angle is $U^2 \simeq l_{\text{min}}/c\tau_{N,U^2=1}\gamma_N \approx 6 \cdot 10^{-8}$, where we used the results of [51] for τ_N and $E_N = 1$ TeV. The number of events is thus

$$N_N^{(W)} \Big|_{m_N=m_{B_c}}^{c\tau_N \gamma_N=l_{\text{min}}} = N_W \times \epsilon_{\text{geom},N}^{(W)} \times \text{Br}(W \rightarrow N) \times P_{\text{decay}}(c\tau_N \gamma_N = l_{\text{min}}) < 1, \quad (4.10)$$

where we have used $\epsilon_{\text{geom},N}^{(W)}$ from Table 3.

5 Results and discussion

Using Eq. (4.1) and requiring $N_{\text{events}} > 3$, corresponding to 95% C.L. in the background free-regime of observing 1 event, we obtain the sensitivity of FACET and FASER2 to HNLs and Higgs-like scalars shown in Fig. 1.

The results agree with the estimates from Sec. 4. Namely, as compared to FASER2, detectors of FACET covers $\simeq 3$ larger solid angle, while the decay volume of FACET is $\simeq 4$ times longer and located $\simeq 5$ times closer. Because of this, for dark scalars, FACET may probe the whole mass range $m_S < m_h/2$, while at FASER2 it is impossible to search for scalars in the mass range $m_B - m_\pi < m_S \lesssim 45$ GeV due to the suppression of the geometric acceptance (see the discussion in Sec. 4.1.2). For HNLs, FACET may probe masses up to $m_N \simeq 6$ GeV, while FASER2 only up to $\simeq 4$ GeV, which is again due both to better sensitivity of FACET at the lower and upper bounds.

As a cross-check of our results, we compare the sensitivity to dark scalars obtained in this work with [17], which used FORESEE package [59]. Namely, we compared the sensitivities of FASER2 to scalars with zero quartic coupling, and the sensitivities of FACET assuming $\text{Br}(h \rightarrow SS) = 0.05$, see Fig. 8. The sensitivities agree well for low masses $m_S \lesssim 10$ GeV, but disagree by a factor of 2-3 at higher masses. The differences may be due to smaller decay width in [17] (which explains the discrepancy at the upper bound) and the absence of the decay acceptance in their estimates.

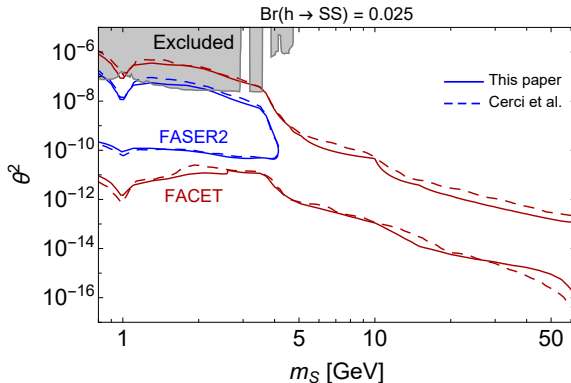


Figure 8. Comparison of the sensitivity of FACET to dark scalars obtained in our work and in [17], assuming $\text{Br}(h \rightarrow SS) = 0.025$ (for FACET) and $\text{Br}(h \rightarrow SS) = 0$ (for FASER2).

An important feature shown in Fig. 1 is that the sensitivity of FACET at the upper bound is better than the sensitivity of other experiments. The reason is the following: the upper bound is controlled by the ratio $\langle p \rangle / l_{\text{min}}$, where $\langle p \rangle$ is the mean momentum of decaying particles, and l_{min} is the distance from the production point to the decay volume. While FACET has l_{min} comparable to experiments such as

SHiP and MATHUSLA, $\langle p \rangle$ is much higher – $\simeq 10$ times higher than at SHiP, and $\simeq 100$ times higher than at MATHUSLA.

6 Conclusions

In this paper, we have estimated the potential of FACET, an experiment located in the far-forward direction at the LHC, to probe new physics, considering the models of scalar and fermion portals as an example. Using semi-analytic estimates, we have compared it with another proposed far-forward experiment, FASER2, see Sec. 4. FACET has a larger decay volume, allowing it to probe the parameter space of long-lived particles, and is located closer to the interaction point (Table 1), which allows searching for short-lived particles. The combination of these features improves the sensitivity compared to FASER2, significantly extending the probed mass range for both models, see Fig. 1. In particular, for dark scalars that are produced by decays of Higgs bosons, FACET may probe the whole kinematically allowed mass range $m_S < m_h/2$, whereas FASER2 has no sensitivity at scalar masses $m_S \lesssim 45$ GeV. For HNLs, FACET may probe masses up to the kinematic threshold for the production from B_c mesons, while FASER2 has the sensitivity limited by $m_N \simeq 4$ GeV.

In addition, FACET is complementary to other LHC-based experiments (such as MATHUSLA) and SHiP. Indeed, the latter may search for new physics particles with much smaller mixing angles due to larger geometrical acceptance and decay volume. FACET, on the other hand, is better suited for probing particles with large couplings due to its on-axis placement: particles produced in the far-forward direction at the LHC have large γ factors, which significantly increases their lifetime and makes it possible to reach the decay volume before decaying.

Acknowledgements

This project has received support from the European Union’s Horizon 2020 research and innovation programme under the Marie Skłodowska-Curie grant agreements No 860881-HIDDeN and 694896. KB is partly funded by the INFN PD51 INDARK grant.

A Mixing and quartic coupling at the lower bound of the sensitivity

Below the B meson mass, scalars may be produced by decays $h \rightarrow S + S, B \rightarrow X_s + S + S$, mediated by the quartic coupling, and $B \rightarrow X_s + S$ mediated by the mixing. Let us establish which of the production channels determines the lower bound of the sensitivity. Namely, let us compare the numbers of scalars produced by decays of h and B in the direction of the FACET experiment:

$$\frac{N_{\text{prod}}(B \rightarrow S)}{N_{\text{prod}}(h \rightarrow SS)} \sim \frac{N_B \cdot \chi_S^{(B)} \text{Br}(B \rightarrow S) \cdot \epsilon_{\text{geom},S}^{(B)}}{N_h \cdot \chi_S^{(h)} \text{Br}(h \rightarrow SS) \cdot \epsilon_{\text{geom},S}^{(h)}} \simeq \begin{cases} \mathcal{O}(1) \cdot \frac{0.05}{\text{Br}(h \rightarrow SS)} \frac{\text{Br}(B \rightarrow X_s S)}{3\theta^2} \frac{\theta^2}{10^{-10}}, & B \rightarrow X_s S \\ \mathcal{O}(10) \frac{\text{Br}(B \rightarrow X_s SS)}{5 \cdot 10^{-10}} & B \rightarrow X_s SS, \end{cases} \quad (\text{A.1})$$

where we have normalized the branching ratios $\text{Br}(B \rightarrow X_s S), \text{Br}(B \rightarrow X_s SS)$ by their characteristic values, see [25]. We conclude that below the kinematic threshold for $B \rightarrow X_s SS$, the lower bound is determined by the quartic production from B , whereas above there are two competing contributions from the mixing production from B and quartic from h .

References

- [1] S. Alekhin et al., *A facility to Search for Hidden Particles at the CERN SPS: the SHiP physics case*, *Rept. Prog. Phys.* **79** (2016), no. 12 124201, [[arXiv:1504.04855](#)].
- [2] P. Agrawal et al., *Feebly-interacting particles: FIPs 2020 workshop report*, *Eur. Phys. J. C* **81** (2021), no. 11 1015, [[arXiv:2102.12143](#)].
- [3] **SHiP** Collaboration, M. Anelli et al., *A facility to Search for Hidden Particles (SHiP) at the CERN SPS*, [arXiv:1504.04956](#).
- [4] **DUNE** Collaboration, R. Acciarri et al., *Long-Baseline Neutrino Facility (LBNF) and Deep Underground Neutrino Experiment (DUNE): Conceptual Design Report, Volume 2: The Physics Program for DUNE at LBNF*, [arXiv:1512.06148](#).
- [5] W. Baldini et al., *SHADOWS (Search for Hidden And Dark Objects With the SPS)*, [arXiv:2110.08025](#).
- [6] **NA62** Collaboration, E. Cortina Gil et al., *The Beam and detector of the NA62 experiment at CERN*, *JINST* **12** (2017), no. 05 P05025, [[arXiv:1703.08501](#)].
- [7] D. Curtin et al., *Long-Lived Particles at the Energy Frontier: The MATHUSLA Physics Case*, *Rept. Prog. Phys.* **82** (2019), no. 11 116201, [[arXiv:1806.07396](#)].
- [8] G. Aielli et al., *Expression of interest for the CODEX-b detector*, *Eur. Phys. J. C* **80** (2020), no. 12 1177, [[arXiv:1911.00481](#)].

- [9] M. Bauer, O. Brandt, L. Lee, and C. Ohm, *ANUBIS: Proposal to search for long-lived neutral particles in CERN service shafts*, [arXiv:1909.13022](#).
- [10] V. V. Gligorov, S. Knapen, B. Nachman, M. Papucci, and D. J. Robinson, *Leveraging the ALICE/L3 cavern for long-lived particle searches*, *Phys. Rev. D* **99** (2019), no. 1 015023, [[arXiv:1810.03636](#)].
- [11] **FASER** Collaboration, A. Ariga et al., *Technical Proposal for FASER: ForwArd Search ExpeRiment at the LHC*, [arXiv:1812.09139](#).
- [12] **FASER** Collaboration, A. Ariga et al., *FASER: ForwArd Search ExpeRiment at the LHC*, [arXiv:1901.04468](#).
- [13] **FASER** Collaboration, H. Abreu et al., *Detecting and Studying High-Energy Collider Neutrinos with FASER at the LHC*, *Eur. Phys. J. C* **80** (2020), no. 1 61, [[arXiv:1908.02310](#)].
- [14] **FASER** Collaboration, H. Abreu et al., *Technical Proposal: FASERnu*, [arXiv:2001.03073](#).
- [15] **SHiP** Collaboration, C. Ahdida et al., *SND@LHC*, [arXiv:2002.08722](#).
- [16] J. L. Feng et al., *The Forward Physics Facility at the High-Luminosity LHC*, [arXiv:2203.05090](#).
- [17] S. Cerci et al., *FACET: A new long-lived particle detector in the very forward region of the CMS experiment*, [arXiv:2201.00019](#).
- [18] M. Du, R. Fang, Z. Liu, and V. Q. Tran, *Enhanced long-lived dark photon signals at lifetime frontier detectors*, *Phys. Rev. D* **105** (2022), no. 5 055012, [[arXiv:2111.15503](#)].
- [19] W. Liu, J. Li, J. Li, and H. Sun, *Testing the seesaw mechanisms via displaced right-handed neutrinos from a light scalar at the HL-LHC*, *Phys. Rev. D* **106** (2022), no. 1 015019, [[arXiv:2204.03819](#)].
- [20] A. Kachanovich, U. Nierste, and I. Nišandžić, *Higgs portal to dark matter and $B \rightarrow K^{(*)}$ decays*, *Eur. Phys. J. C* **80** (2020), no. 7 669, [[arXiv:2003.01788](#)].
- [21] A. Filimonova, R. Schäfer, and S. Westhoff, *Probing dark sectors with long-lived particles at BELLE II*, *Phys. Rev. D* **101** (2020), no. 9 095006, [[arXiv:1911.03490](#)].
- [22] M. Drewes and J. Hajer, *Heavy Neutrinos in displaced vertex searches at the LHC and HL-LHC*, *JHEP* **02** (2020) 070, [[arXiv:1903.06100](#)].
- [23] A. M. Abdullahi et al., *The Present and Future Status of Heavy Neutral Leptons*, in *2022 Snowmass Summer Study*, 3, 2022. [arXiv:2203.08039](#).
- [24] F. Bezrukov and D. Gorbunov, *Light inflaton Hunter's Guide*, *JHEP* **05** (2010) 010, [[arXiv:0912.0390](#)].
- [25] I. Boiarska, K. Bondarenko, A. Boyarsky, V. Gorkavenko, M. Ovchinnikov, and A. Sokolenko, *Phenomenology of GeV-scale scalar portal*, *JHEP* **11** (2019) 162, [[arXiv:1904.10447](#)].

- [26] C. Bird, P. Jackson, R. V. Kowalewski, and M. Pospelov, *Search for dark matter in $b \rightarrow s$ transitions with missing energy*, *Phys. Rev. Lett.* **93** (2004) 201803, [[hep-ph/0401195](#)].
- [27] B. Batell, M. Pospelov, and A. Ritz, *Multi-lepton Signatures of a Hidden Sector in Rare B Decays*, *Phys. Rev.* **D83** (2011) 054005, [[arXiv:0911.4938](#)].
- [28] J. D. Clarke, R. Foot, and R. R. Volkas, *Phenomenology of a very light scalar ($100 \text{ MeV} \leq m_h \leq 10 \text{ GeV}$) mixing with the SM Higgs*, *JHEP* **02** (2014) 123, [[arXiv:1310.8042](#)].
- [29] K. Schmidt-Hoberg, F. Staub, and M. W. Winkler, *Constraints on light mediators: confronting dark matter searches with B physics*, *Phys. Lett.* **B727** (2013) 506–510, [[arXiv:1310.6752](#)].
- [30] J. A. Evans, *Detecting Hidden Particles with MATHUSLA*, *Phys. Rev.* **D97** (2018), no. 5 055046, [[arXiv:1708.08503](#)].
- [31] F. Bezrukov, D. Gorbunov, and I. Timiryasov, *Uncertainties of hadronic scalar decay calculations*, [[arXiv:1812.08088](#)].
- [32] A. Monin, A. Boyarsky, and O. Ruchayskiy, *Hadronic decays of a light Higgs-like scalar*, *Phys. Rev.* **D99** (2019), no. 1 015019, [[arXiv:1806.07759](#)].
- [33] M. W. Winkler, *Decay and detection of a light scalar boson mixing with the Higgs boson*, *Phys. Rev.* **D99** (2019), no. 1 015018, [[arXiv:1809.01876](#)].
- [34] C. Frugiuele, E. Fuchs, G. Perez, and M. Schlaffer, *Relaxion and light (pseudo)scalars at the HL-LHC and lepton colliders*, *JHEP* **10** (2018) 151, [[arXiv:1807.10842](#)].
- [35] A. J. Helmboldt and M. Lindner, *Prospects for three-body Higgs boson decays into extra light scalars*, *Phys. Rev.* **D95** (2017), no. 5 055008, [[arXiv:1609.08127](#)].
- [36] M. B. Voloshin, *Once Again About the Role of Gluonic Mechanism in Interaction of Light Higgs Boson with Hadrons*, *Sov. J. Nucl. Phys.* **44** (1986) 478. [*Yad. Fiz.*44,738(1986)].
- [37] S. Raby and G. B. West, *The Branching Ratio for a Light Higgs to Decay Into $\mu^+\mu^-$ Pairs*, *Phys. Rev.* **D38** (1988) 3488.
- [38] T. N. Truong and R. S. Willey, *Branching Ratios for Decays of Light Higgs Bosons*, *Phys. Rev.* **D40** (1989) 3635.
- [39] J. F. Donoghue, J. Gasser, and H. Leutwyler, *The Decay of a Light Higgs Boson*, *Nucl. Phys.* **B343** (1990) 341–368.
- [40] R. S. Willey and H. L. Yu, *The Decays $K^\pm \rightarrow \pi^\pm \ell^+ \ell^-$ and Limits on the Mass of the Neutral Higgs Boson*, *Phys. Rev.* **D26** (1982) 3287.
- [41] R. S. Willey, *Limits on Light Higgs Bosons From the Decays $K^\pm \rightarrow \pi^\pm \ell^- \ell^+$* , *Phys. Lett.* **B173** (1986) 480–484.
- [42] B. Grzadkowski and P. Krawczyk, *HIGGS PARTICLE EFFECTS IN FLAVOR CHANGING TRANSITIONS*, *Z. Phys.* **C18** (1983) 43–45.

- [43] H. Leutwyler and M. A. Shifman, *Light Higgs Particle in Decays of K and η Mesons*, *Nucl. Phys.* **B343** (1990) 369–397.
- [44] H. E. Haber, A. S. Schwarz, and A. E. Snyder, *Hunting the Higgs in B Decays*, *Nucl. Phys.* **B294** (1987) 301–320.
- [45] R. S. Chivukula and A. V. Manohar, *LIMITS ON A LIGHT HIGGS BOSON*, *Phys. Lett.* **B207** (1988) 86. [Erratum: *Phys. Lett.*B217,568(1989)].
- [46] **CMS** Collaboration, A. M. Sirunyan et al., *Search for invisible decays of a Higgs boson produced through vector boson fusion in proton-proton collisions at $\sqrt{s} = 13$ TeV*, *Phys. Lett.* **B793** (2019) 520–551, [[arXiv:1809.05937](https://arxiv.org/abs/1809.05937)].
- [47] **ATLAS** Collaboration, M. Aaboud et al., *Search for invisible Higgs boson decays in vector boson fusion at $\sqrt{s} = 13$ TeV with the ATLAS detector*, *Phys. Lett.* **B793** (2019) 499–519, [[arXiv:1809.06682](https://arxiv.org/abs/1809.06682)].
- [48] P. Bechtle, S. Heinemeyer, O. Stål, T. Stefaniak, and G. Weiglein, *Probing the Standard Model with Higgs signal rates from the Tevatron, the LHC and a future ILC*, *JHEP* **11** (2014) 039, [[arXiv:1403.1582](https://arxiv.org/abs/1403.1582)].
- [49] I. Boiarska, K. Bondarenko, A. Boyarsky, M. Ovchinnikov, O. Ruchayskiy, and A. Sokolenko, *Light scalar production from Higgs bosons and FASER 2*, *JHEP* **05** (2020) 049, [[arXiv:1908.04635](https://arxiv.org/abs/1908.04635)].
- [50] K. Bondarenko, A. Boyarsky, M. Ovchinnikov, and O. Ruchayskiy, *Sensitivity of the intensity frontier experiments for neutrino and scalar portals: analytic estimates*, *JHEP* **08** (2019) 061, [[arXiv:1902.06240](https://arxiv.org/abs/1902.06240)].
- [51] K. Bondarenko, A. Boyarsky, D. Gorbunov, and O. Ruchayskiy, *Phenomenology of GeV-scale Heavy Neutral Leptons*, *JHEP* **11** (2018) 032, [[arXiv:1805.08567](https://arxiv.org/abs/1805.08567)].
- [52] **Particle Data Group** Collaboration, R. L. Workman and Others, *Review of Particle Physics*, *PTEP* **2022** (2022) 083C01.
- [53] M. Cepeda et al., *Report from Working Group 2: Higgs Physics at the HL-LHC and HE-LHC*, *CERN Yellow Rep. Monogr.* **7** (2019) 221–584, [[arXiv:1902.00134](https://arxiv.org/abs/1902.00134)].
- [54] M. Cacciari, M. Greco, and P. Nason, *The $P(T)$ spectrum in heavy flavor hadroproduction*, *JHEP* **05** (1998) 007, [[hep-ph/9803400](https://arxiv.org/abs/hep-ph/9803400)].
- [55] M. Cacciari, S. Frixione, and P. Nason, *The $p(T)$ spectrum in heavy flavor photoproduction*, *JHEP* **03** (2001) 006, [[hep-ph/0102134](https://arxiv.org/abs/hep-ph/0102134)].
- [56] M. Cacciari, S. Frixione, N. Houdeau, M. L. Mangano, P. Nason, and G. Ridolfi, *Theoretical predictions for charm and bottom production at the LHC*, *JHEP* **10** (2012) 137, [[arXiv:1205.6344](https://arxiv.org/abs/1205.6344)].
- [57] M. Cacciari, M. L. Mangano, and P. Nason, *Gluon PDF constraints from the ratio of forward heavy-quark production at the LHC at $\sqrt{S} = 7$ and 13 TeV*, *Eur. Phys. J.* **C75** (2015), no. 12 610, [[arXiv:1507.06197](https://arxiv.org/abs/1507.06197)].
- [58] **ATLAS** Collaboration, M. Aaboud et al., *Measurement of the $W^\pm Z$ boson*

pair-production cross section in pp collisions at $\sqrt{s} = 13$ TeV with the ATLAS Detector, *Phys. Lett. B* **762** (2016) 1–22, [[arXiv:1606.04017](#)].

- [59] F. Kling and S. Trojanowski, *Forward experiment sensitivity estimator for the LHC and future hadron colliders*, *Phys. Rev. D* **104** (2021), no. 3 035012, [[arXiv:2105.07077](#)].
- [60] T. Asaka, S. Blanchet, and M. Shaposhnikov, *The nuMSM, dark matter and neutrino masses*, *Phys. Lett. B* **631** (2005) 151–156, [[hep-ph/0503065](#)].
- [61] T. Asaka and M. Shaposhnikov, *The ν MSM, dark matter and baryon asymmetry of the universe*, *Phys. Lett. B* **620** (2005) 17–26, [[hep-ph/0505013](#)].